

RESEARCH

Open Access



Identification of lncRNAs involved in the hair follicle cycle transition of cashmere goats in response to photoperiod change

Min Yang^{1†}, Yingying Li^{1†}, Qianqian Liang¹, Huajiao Dong¹, Yuehui Ma², Göran Andersson³, Erik Bongcam-Rudloff³, Hafiz Ishfaq Ahmad⁴, Xuefeng Fu⁵ and Jilong Han^{1*}

Abstract

Background Cashmere goats, as one of the important domesticated animal species, are known for their high-quality fiber. The growth of cashmere has seasonal variations caused by photoperiodic changes, but the molecular genetic mechanisms underlying this phenotype including the functional role of long non-coding RNAs (lncRNA) is still poorly understood.

Results In this study, we analyzed the RNA-seq dataset of 39 Cashmere goat skin samples including all different growth stages and identified 1591 lncRNAs. These lncRNAs exhibited growth stage-specific expression patterns. Combining shortened light and hair follicle growth cycles, we found that 68% of differentially photo-responsive lncRNAs showed similar expression trends during transition phase I (early anagen to anagen phase). This suggests that the mechanism of light-controlled induction of hair follicles from early anagen to anagen is similar to that of transition phase I. According to weighted gene co-expression network analyses (WGCNA) analysis, it was found that two gene clusters and 10 hub lncRNAs participated in the transformation of hair follicle cycle, inducing hair follicles to enter the full growth phase in advance. These hub lncRNAs may regulate the development cycle of hair follicles through cis- or trans-regulation on clock genes, SLC superfamily genes, fibroblast growth factor genes.

Conclusions This study identified the key lncRNAs and target genes probably participating in the transformation of hair follicle cycle. This study will help further elucidate the role of lncRNAs in the hair follicle cycle and development.

Keywords Cashmere goat, lncRNA, Shortened photoperiod, Hair follicle cycle, WGCNA, Transcriptomic analysis

[†]Min Yang and Yingying Li contributed equally to this work.

*Correspondence:

Jilong Han

hanjilong@shzu.edu.cn

¹College of Animal Science and Technology, Shihezi University, Shihezi 832061, China

²Institute of Animal Sciences, Chinese Academy of Agricultural Sciences, Beijing 100193, China

³Department of Animal Biosciences, Swedish University of Agricultural Sciences, 75007 Uppsala, Sweden

⁴Department of Animal Breeding and Genetics, Faculty of Veterinary and Animal Sciences, Islamia University of Bahawalpur, Bahawalpur 63100, Pakistan

⁵Institute of Animal Science, Xinjiang Academy of Animal Sciences, Urumqi 830011, China



Background

Hair follicles (HFs), being crucial skin appendages in mammals, exhibit intricate structures and comprise various components [1]. The HF, a miniature organ resulting from the interplay between the epidermis and dermis, undergoes a cyclical growth process throughout the mammal's lifespan [2]. Typically, the HF growth cycle involves distinct phases: growth (anagen), regression (catagen), and quiescence (telogen), each accompanied by specific morphological transformations. Nevertheless, the pattern of HF growth cycles varies among species. For instance, human HF growth is asynchronous, with each HF cycling independently, whereas mice display more synchronized cycling [3]. The growth of cashmere in Cashmere goats follows an annual cycle influenced by changes in photoperiod. For the Inner Mongolia Cashmere Goat, the anagen phase lasts eight months, from May to December. The catagen phase occurs from January to March, while April is designated as the telogen phase [4–5]. Various factors, including age, climate, environment, and health status, can influence the progression and timing of these three stages of the HF growth cycle [6]. Furthermore, the morphogenesis and cycling of HFs are regulated by multiple signaling pathways, such as WNT and BMP signaling pathways [7]. Despite this understanding, the involvement of long non-coding RNAs (lncRNAs) in controlling the HF cycle remains inadequately described.

Cashmere goats, as one of the important domesticated animal species, possess two types of hair follicles in their skin: primary hair follicles (PHFs) and secondary hair follicles (SHFs) [8]. Cashmere, the valuable fiber, is produced by the SHFs. The growth of cashmere exhibits a seasonal pattern arising from photoperiod change. Unlike many other animals, the secondary hair follicle cycle of Cashmere goat is just one year, making them an excellent model for studying the impact of seasonal cycles and photoperiod changes on the HF growth cycle. Photoperiod is considered the most dominant environmental cue allowing animals to anticipate and adapt to seasonal changes [9]. As one of the key environmental factors, photoperiod has direct effects on the circadian clock, which, in turn, affects the growth of HF [10]. The circadian clock has a substantial influence on the HF cycle, both *in vitro* and *in vivo* [11]. Research has indicated that red light at 650 nm can stimulate the proliferation of human HF cells and markedly delay the transition of hair follicles from anagen to telogen [12]. In Cashmere goat, studies have demonstrated that artificially shortening the photoperiod can extend the cashmere growth period [13]. However, the molecular mechanism, particularly the epigenetic aspects, underlying the effects of seasonal cycles and photoperiod changes on the HF growth cycle remain unclear.

Long non-coding RNA (lncRNA) is a kind of non-coding RNA with a length of more than 200 nt, which is widely found in animal and plant cells [14]. lncRNA represent relatively newly defined classes of regulatory RNA molecules whose functions and importance are only beginning to be elucidated in a wide range of organisms [15]. With the application and continuous development of the new generation of high-throughput sequencing technology, more and more lncRNAs in organisms have been continuously discovered. According to their position in the genome, lncRNAs can be divided into five categories: sense lncRNAs, antisense lncRNAs, bidirectional lncRNAs, intronic lncRNAs, and intergenic lncRNAs. lncRNAs are important components of the mammalian transcriptome and regulate gene expression at multiple levels. They are involved in many life activities such as modulating chromatin structure through epigenetic regulation, growth and development, immunity and metabolism [16]. Recent comprehensive research has highlighted the expression of non-coding RNAs in mammalian hair follicles, playing a crucial role in regulating hair follicle development and regeneration. Long non-coding RNAs (lncRNAs) also exhibit widespread involvement in regulating hair follicle growth [17]. lncRNAs have been found to regulate hair follicle cycling in Cashmere goats [18–19], sheep [20], Rabbit [21] and Yak [22]. However, the specific functional roles of these lncRNAs in controlling the hair follicle cycle based on seasonal cycles and photoperiod changes have not been well described. In this study, Cashmere goat subjected to different seasons and controlled photoperiods were investigated in an effort to elucidate the key long non-coding RNAs and their different classifications of lncRNAs involved in the transition of the hair follicle cycle, which will contribute to a better understanding of the molecular mechanisms governing the hair follicle cycle.

Methods

The tissue samples and RNA-seq sequencing data

This experiment was performed at the Cashmere goat farm, located in the Inner Mongolia Autonomous Region of China (latitude 38°23'N, longitude 108°07'E, altitude 1,378 m). These goats were raised in a shared environment with unrestricted access to food and water. No animals were sacrificed as part of this research, and all procedures, including sample collection, were non-invasive and conducted in compliance with animal welfare guidelines. The skin samples were collected according to our previous study [5], with the details as follows: after depilation of the scapular hair and administration of local anesthesia to each goat, a 1 cm² skin sample was taken using sterile ophthalmic scissors from the scapular. Half was stored in RNAlater (Termo Fisher Scientific, USA) for RNA extraction, and the other half was stored in 4%

paraformaldehyde fixation solution to prepare paraffin sections. Yunnan Baiyao hemostatic powder (Yunnan Baiyao Group Co., Ltd., China) was evenly applied to the wound of skin. The RNA-seq data used in this study was obtained from a previous work [5, 18], a total of 39 samples were collected at seven different months (January, April, May, June, August, September, and October), comprising 20 pairs of control and light-treated groups. The dataset encompasses all stages of hair follicle development, including the early anagen, anagen, catagen, and telogen (Table S1).

Read alignment and transcriptome assembly

The goat reference genome sequence file and goat reference genome annotation file were acquired from the NCBI website (https://ftp.ncbi.nlm.nih.gov/genomes/refs_eq/vertebrate_mammalian/Capra_hircus/latest_assembly_versions/GCF_001704415.2_ARS1.2/). Clean reads were aligned to the goat genome using Hisat2 [23] with default settings. Subsequently, the aligned reads for each sample were sorted based on chromosome order using Samtools. Transcriptome assembly for each sample was performed using StringTie [24] in reference-based mode. The resulting transcripts from all samples were consolidated into a Gene Transfer Format (GTF) file.

Novel lncRNA identification

To identify novel long intergenic non-coding RNAs (lncRNAs), the following steps were employed: First, the assembled transcriptomes of each sample were compared with the goat reference transcriptome GTF file using Cuffcompare [25]. Transcripts assigned with a class code 'u' were selected as putative novel transcripts; Second, transcripts with a length of ≥ 200 bp were retained using a Python script; Third, CPC2 [26] and CNCI [27] were utilized to predict the coding potential of each transcript. Transcripts demonstrating coding potential were subsequently excluded from further analysis; and finally, the transcripts obtained through the above-mentioned methods were considered as candidate lncRNAs for subsequent analysis.

Gene quantification and differential expression analysis

First, the assembled transcripts from all samples were merged into a non-redundant transcriptome using the merge function in the StringTie software. Subsequently, the read counts and FPKM (Fragments Per Kilobase of transcript per Million mapped reads) values of transcripts were calculated for all samples using the built-in quantification script in StringTie. Differential analysis was then conducted for protein-coding genes and lncRNA (long intergenic non-coding RNA) across the 39 transcriptomes using the DESeq2 package [28] in the R software. This analysis was performed based on count values and

resulted in the identification of Differentially Expressed mRNAs (DEMs) and Differentially Expressed lncRNAs (DE lncRNAs). The DESeq2 package was used to normalize gene expression levels across the seven months, with normalization performed only between the two samples being compared. For exploring the effects of photoperiodic regulation on the cyclic changes of hair follicles, the DEG screening thresholds were adjusted to $|\log_2 FC| \geq 0.58$ with $\text{padj} \leq 0.05$.

Weighted Gene Co-expression Network Analysis (WGCNA) and hub lncRNA identification

Weighted Gene Co-expression Network Analysis was performed using the R package WGCNA (version 1.71) [29] to identify modules of co-expressed genes based on the gene expression data from 39 samples. Initially, the soft threshold (β) for network construction was set to 5, and the minimum module size was defined as 30. Clusters with a height less than 0.6 in the merged dendrogram were recognized as key modules. Subsequently, the intramodular connectivity function was employed to compute the connectivity (k_{Within}) of each gene in the entire network. Using k_{Total} (connectivity of each gene based on its r -values to all other genes in the whole network) as the criterion, the top five lncRNAs in the network with the highest correlation to protein-coding genes were identified as hub lncRNAs.

Functional enrichment analysis

Functional enrichment analysis was performed using the web server g:Profiler (<http://biit.cs.ut.ee/gprofiler/>) with default parameters for Gene Ontology (GO) enrichment analysis. Additionally, KEGG pathway enrichment analysis was conducted using the ClueGO plugin in CytoScape (version 3.91) [30]. The criterion for pathway selection was set to genes enriching in pathways with a proportion greater than 2%.

Pathway mRNA-lncRNA network construction

KEGG enrichment analysis was performed on genes within key modules, and those enriched in crucial signaling pathways were carefully selected. Subsequently, a pathway-mRNA-lncRNA network was constructed, utilizing the top five co-expressed lncRNA genes as targets. The network was visualized using CytoScape [31].

Prediction of lncRNA target genes

For cis-target gene prediction, we identified differentially expressed protein-coding genes located within 100 kb upstream and downstream of a lncRNA locus, based on their genomic positions. For trans-target gene prediction, Pearson correlation coefficients were computed using expression matrices of Differentially Expressed lncRNAs (DEL) and Differentially Expressed mRNAs

(DEMs), employing FPKM values. Trans-target genes were defined as DEMs with Pearson correlation coefficients exceeding 0.90.

Validation of RNA-seq data by reverse transcription quantitative real-time PCR (RT-qPCR)

To confirm the reliability of the RNA-seq dataset used in this study, six protein-coding mRNAs and six lncRNAs were randomly selected for RT-qPCR validation. Primers were designed using the Primer3 software, and their specificity was verified using NCBI's Primer-Blast. The primers were synthesized by GenScript Biotechnology Co. Ltd., with β -actin (GenBank accession number: NM_001314342.1) used as the internal reference (Table S2). RNA was extracted from skin samples collected from the shoulder region of adult Cashmere goats in January, April, and September, using an RNA extraction kit (Define this kit). The reverse transcription reaction was performed using the TransGen Biotech reverse transcription kit (EasyScript® One-step gDNA Removal and cDNA Synthesis SuperMix) according to the manufacturer's instructions. The reaction volume was 20 μ L, with a total RNA input of 1 ng. The reaction conditions were set at 42 °C for 15 min and 85 °C for 5 s to obtain cDNA. RT-qPCR reactions were prepared using the ArtiCanATM SYBR qPCR Mix according to the manufacturer's instructions. The reaction mixture included 10 μ L of RT-qPCR Mix, 0.4 μ L of each upstream and downstream primer, 0.1 μ g of cDNA template, and ddH₂O to a final volume of 20 μ L. The RT-qPCR amplification program consisted of an initial denaturation at 95 °C for 60 s, followed by 45 cycles of denaturation at 95 °C for 10 s, annealing at 60 °C for 20 s, and extension at 72 °C for 20 s. A melting curve analysis was performed by increasing the temperature from 95 °C to 65 °C, with a 1 s hold at each temperature step. Each sample was run with three biological replicates. The $2^{-\Delta\Delta C_t}$ method was used for data analysis [32]. The results were presented as mean \pm standard deviation (SD). Statistical analyses, including Student's *t*-test and correlation analysis, were conducted using Graph Prism 9 software (ns, $p > 0.05$; *, $p < 0.05$; **, $p < 0.01$; ***, $p < 0.001$).

Results

The Identification of lncRNA

A total of 1033.35 million high-quality clean reads representing seven different months spanning the entire hair follicle growth cycle of Cashmere goat were obtained. The average number of clean reads per sample was 2,870 million, making them suitable for subsequent analysis. The alignment rate for individual samples ranged from 96.21 to 97.97%, with an average alignment rate of 97.51% (Table S1). This indicates that the majority of sequencing reads are valid, and total RNA contamination is negligible. After filtering based on lncRNA length, exon count,

and coding potential, a total of 1,071,895 transcripts were obtained. Among these, 1,591 candidate Long Non-Coding RNAs (lncRNA) were identified (Fig. 1A, Table S3). The number of alternative spliced transcripts for majority lncRNAs and mRNAs is 1 (Fig. 1B). However, in contrast to protein-coding genes, lncRNAs exhibit shorter transcript lengths (Fig. 1C). Furthermore, lncRNAs, on average, display lower overall expression levels compared to mRNAs (Fig. 1D). In summary, the features of the identified lncRNAs through this process align with previously published characteristics of lncRNAs, validating the effectiveness of our pipeline.

Natural seasonal cycle specific expression of lncRNA in skin hair follicles

Principal component analysis (PCA) was conducted on all lncRNAs in samples under normal light conditions for seasonal cycle, and the results indicated that samples tended to cluster together during the early anagen, anagen, catagen, and telogen stages (Fig. 2A), consistent with the morphological changes observed in our previous studies [5]. To unravel key factors contributing to the periodicity of HF, data from June, October, January, and April were selected to represent the early anagen, anagen, catagen, and telogen stages, respectively. This allowed for the analysis of differential genes during the four transitional phases: Transition I (early anagen to anagen), Transition II (anagen to catagen), Transition III (catagen to telogen), Transition IV (telogen to early anagen). The results revealed that quantitative differences in the expression of lncRNAs at different developmental stages, with each stage having over 1,000 lncRNAs. The anagen phase displayed the highest number, while the early anagen phase exhibited the fewest (Fig. 2B), highlighting stage-specific expression patterns of lncRNAs. Moreover, a total of 3,412 differentially expressed mRNAs (DEMs) and 244 differentially expressed lncRNAs (DELs) were screened (Table S4), with the fewest differential genes in Transition II and the most in Transition I (Fig. 2C, D). A heatmap visually represented the expression changes of the 244 DELs across the four developmental stages (Fig. 2E). Notably, DELs in the growth and regression phases exhibited opposite expression trends, possibly due to their distinct stages. In the telogen phase, the follicles undergo programmed cell death, while in the anagen phase, follicles undergo continuous reconstruction.

Shortened photoperiod induced expression differences in the HF cycle

To elucidate the lncRNAs impact of shortened light exposure on the hair follicle cycle in Cashmere goats, we performed differential analysis using DESeq2 for each month (January, April, May, June, August, September, and October). A total of 1,378 DEMs and 131 DELs were

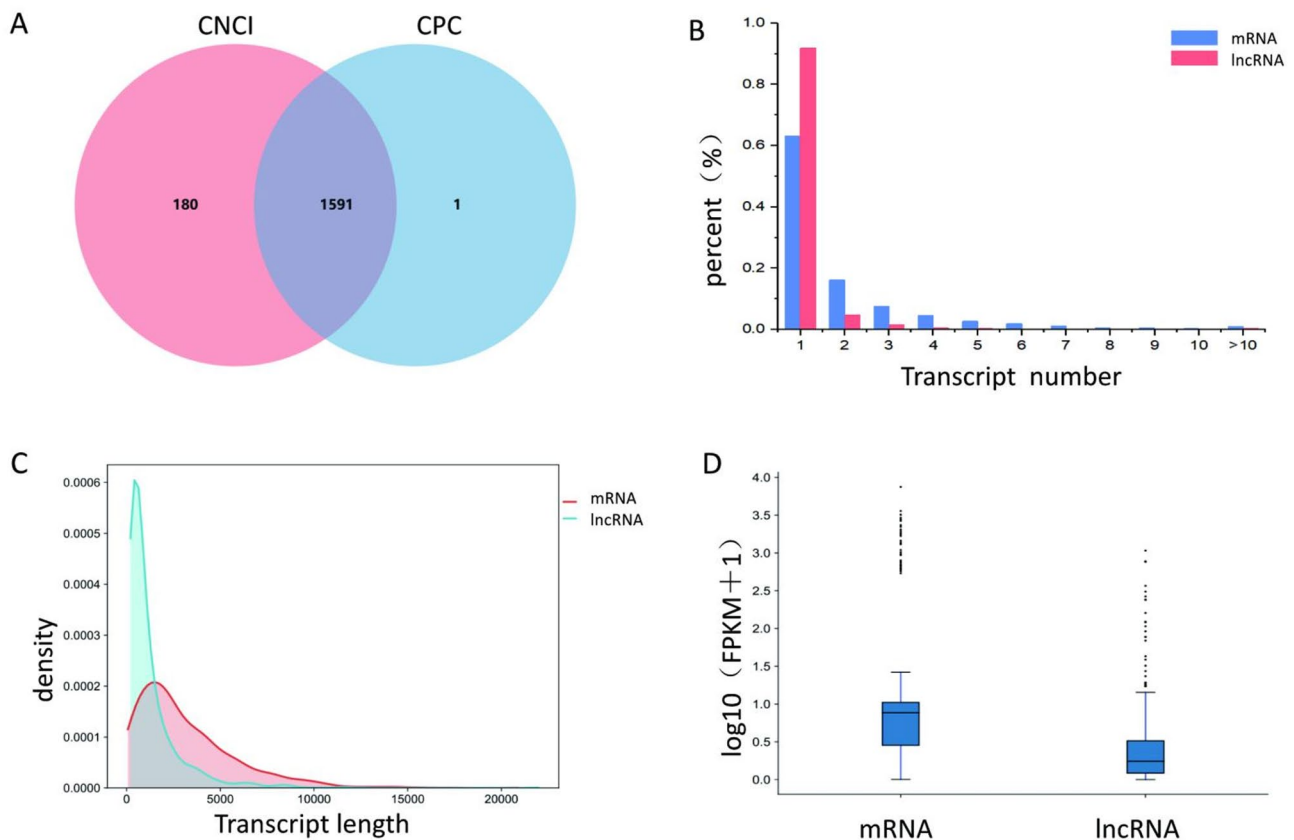


Fig. 1 Features of lncRNA in the skin of Cashmere goat. **(A)** The Venn diagrams depicting the common characteristics between CNCI and CPC methods in the analysis of lncRNA; **(B)** Transcript number distribution in goat skin for lncRNA and mRNA; **(C)** Transcript length distribution of lncRNA and mRNA; **(D)** Expression levels of lncRNA and mRNA

detected between the shortened photoperiod and control groups (Table S5). The month with the highest number of Differentially Expressed Genes (DEGs) was June, with 895 genes (831 DEGs, 64 DELs), and the genes with increased level of RNA expression outnumbered those with decreased gene expression. The number of DEGs for the other months were 95 (January), 107 (April), 461 (May), 145 (August), 94 (September), and 50 (October) (Fig. 3A, B). This result indicates that June is the most critical month for light exposure in regulating cashmere growth. The PCA plot for 39 samples (Fig. 3C) showed that the shortened photoperiod group in June (6e) clustered with anagen samples, while being separated from samples in the early growth period, suggesting that artificial shortening of light exposure can advance the entry of Cashmere goat hair follicles into the growth period. By overlapping DEGs after light exposure with different transition periods under normal light conditions, we found 685 genes (637 DEGs and 48 DELs) (Table S6) that also exhibited a periodic expression pattern, accounting for a high percentage of 76.5% (Fig. 3D). Similarly, 68% of the light-responsive genes showed expression trends consistent with transition I.

Weighted Gene Co-expression Network Analysis (WGCNA) reveals key lncRNA clusters associated with cashmere goat HF development

In order to further explore the potential regulatory roles of lncRNA in different developmental stages of Cashmere goat HF, we conducted WGCNA based on the 685 DEGs exhibiting periodic expression patterns in response to shortened light exposure. The unscaled topological overlap matrix (TOM) results indicated that when the soft-thresholding power (beta) was set to 5, the TOM fit curve remained unchanged, and the mean connectivity of each gene module became smaller (Fig. 4A). Ultimately, three modules were obtained. The heatmap in Fig. 4B illustrates the inter-module correlations, while Fig. 4C depicts the correlation between modules and traits. Two key gene clusters, potentially involved in the HF cycle, were identified. The anagen-enriched module (blue) ($r=0.76$ and $p<0.01$) and a negative correlation with telogen ($r = -0.65$ and $p<0.01$). The early anagen-enriched module (turquoise) ($r=0.74$ and $p<0.01$) and a negative correlation with anagen ($r = -0.62$ and $p<0.01$). The grey module, which is conventionally excluded from downstream functional analyses in WGCNA, contains genes lacking significant co-expression patterns with other clusters.

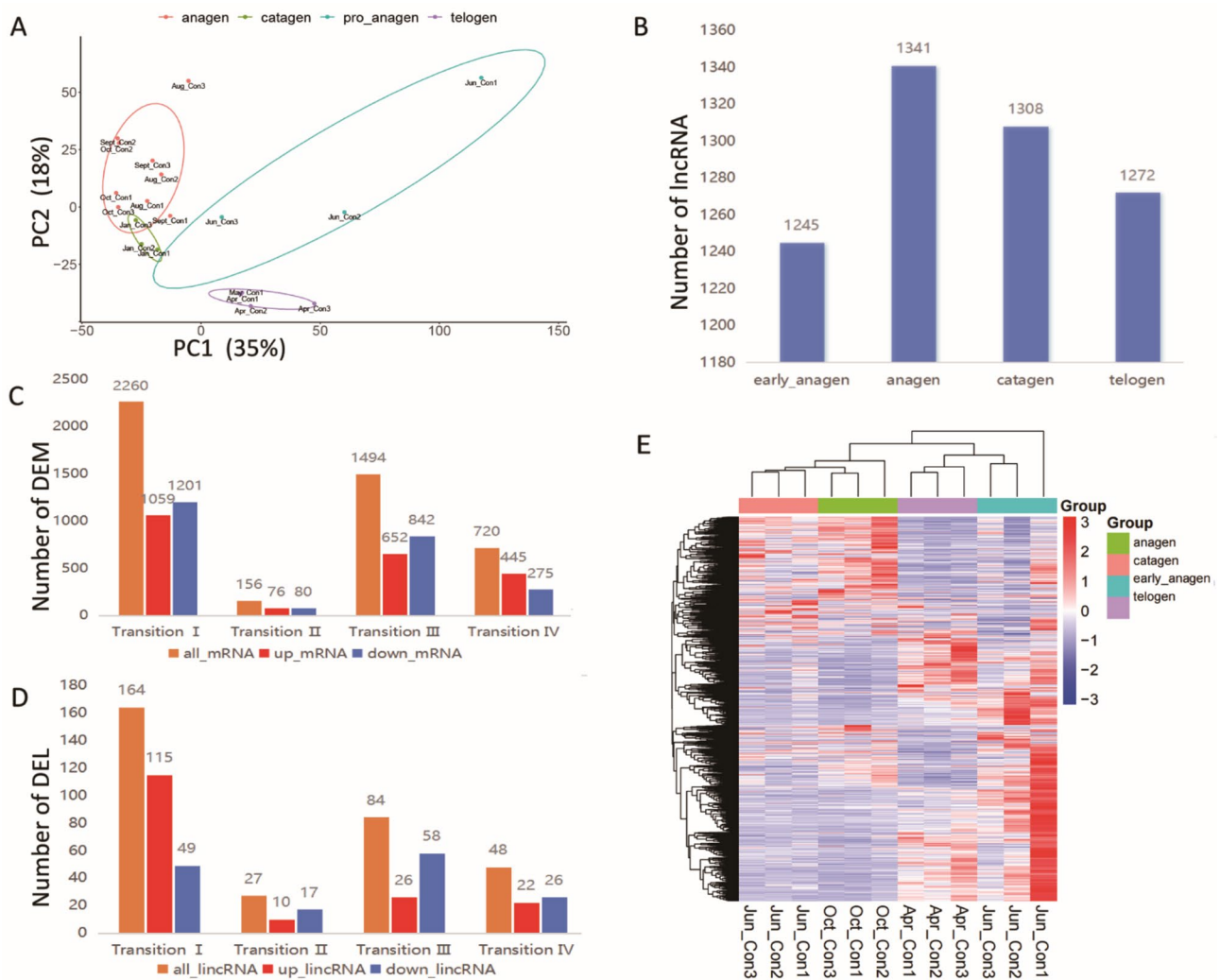


Fig. 2 Stage-specific expression of lncRNA in skin hair follicles. **(A)** PCA plot of all lncRNAs for samples; **(B)** The number of expressed lncRNAs in samples for different months; **(C)** The differentially expressed mRNAs (DEMs) at different stages of hair follicle development; **(D)** The differentially expressed lncRNAs (DELS) at different stages of hair follicle development; **(E)** The heatmap of DELS

Notably, the turquoise module contains the highest number of genes (Fig. 4D). Additional details of the three clusters of genes are listed in Table S7.

Subsequently, we performed GO and KEGG analyses on the blue and turquoise modules (Fig. 5, Table S8). In the blue module, comprising 222 protein-coding genes and 12 lncRNAs, we identified enrichment in 37 KEGG pathways. Notable signaling pathways included the AMPK signaling pathway, TGF- β signaling pathway, along with functional terms like transmembrane transport, organonitrogen compound metabolic process, and cellular response to nutrient among the 15 enriched GO terms. In the turquoise module, comprising 411 protein-coding genes and 35 lncRNAs. The turquoise module participated in 99 KEGG pathways, including ECM-receptor interaction, MAPK, Oxytocin, Jak-STAT, Rap1, PI3K-Akt signaling pathways. The module also

involved 145 GO terms, highlighting terms related to protein synthesis and modification, collagen biosynthesis and modifying enzymes, collagen formation, and positive regulation of protein metabolic process. Additionally, terms associated with cellular development, such as cell differentiation, cellular developmental process, cell migration, cell adhesion, and cell population proliferation, were significantly enriched.

Identification of hub lncRNAs in HF development

An alternative approach to deducing potential functions for lncRNAs involves exploring networks to pinpoint hub genes. Hub genes are those that exhibit functional interconnectedness with numerous other genes, signifying their importance due to their centrality within a network of genes [33]. In this study, we designated the top five lncRNAs with the highest connectivity within

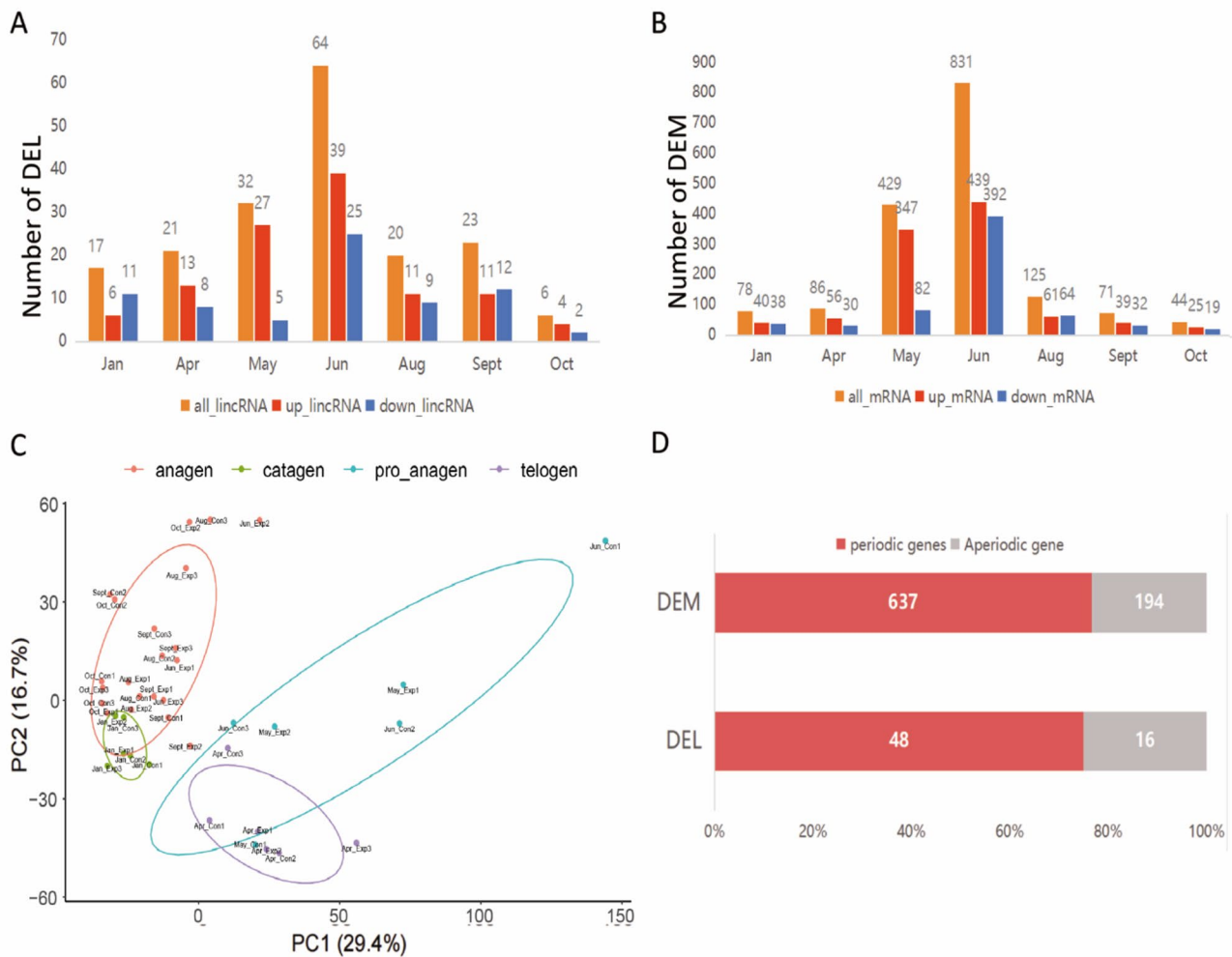


Fig. 3 Analysis of differential expression patterns induced by a shortened photoperiod. **(A)** The number of differentially expressed lincRNAs (DEL) between the shortened photoperiod and the control group; **(B)** The number of differentially expressed mRNAs (DEM) between the shortened photoperiod and the control group; **(C)** PCA analysis results for all samples; **(D)** Proportion of genes showing both a periodic expression pattern and DEG between the shortened photoperiod and the control group in June

each module as hub lincRNAs (Table 1). We selected the top 5 connected lincRNAs in each module and their co-expressed coding genes to construct a pathway-mRNA-lincRNA network (Fig. 6), revealing 83 nodes. (Table S9). The network depicted interactions among 10 Hub lincRNAs, 16 pathways, and 57 mRNAs.

Identification of cis- and trans-targets of hub lincRNAs

lincRNAs can be broadly classified into those that act in cis, influencing the expression and/or chromatin state of nearby genes, and those that execute an array of functions throughout the cell in trans [34]. Based on the positional information of hub lincRNAs, a range was set at 100 k as a boundary, leading to the identification of 26 pairs of cis-regulatory relationships (involving eight hub lincRNAs) (Table S10). Interestingly, three of these lincRNAs were found to be involved in the regulation of hair follicle growth (Table 2). Additionally, we predicted

trans-regulatory relationships of hub lincRNAs by examining expression pattern correlations ($R > 0.95$), revealing 641 pairs of trans-regulatory relationships. Ten hub lincRNAs were identified to regulate 371 DEMs (Table S11). Among them, eight lincRNAs were found to have anti-sense target genes, previously reported to potentially participate in hair follicle regulation (Table 3). Of particular interest is the observation that both cis-acting and trans-acting target genes of *XLOC_009050* and *XLOC_018730* are linked to hair follicle development, with a significant presence of *DLX3* in the regulatory networks of *XLOC_018730*.

Here, we performed functional enrichment analysis on both the cis- and trans-target genes of the hub lincRNAs [42]. These genes were enriched for 43 Gene Ontology (GO) terms related to biological processes, cellular components, and molecular functions (Fig. 6A), primarily focusing on cellular processes, metabolic processes,

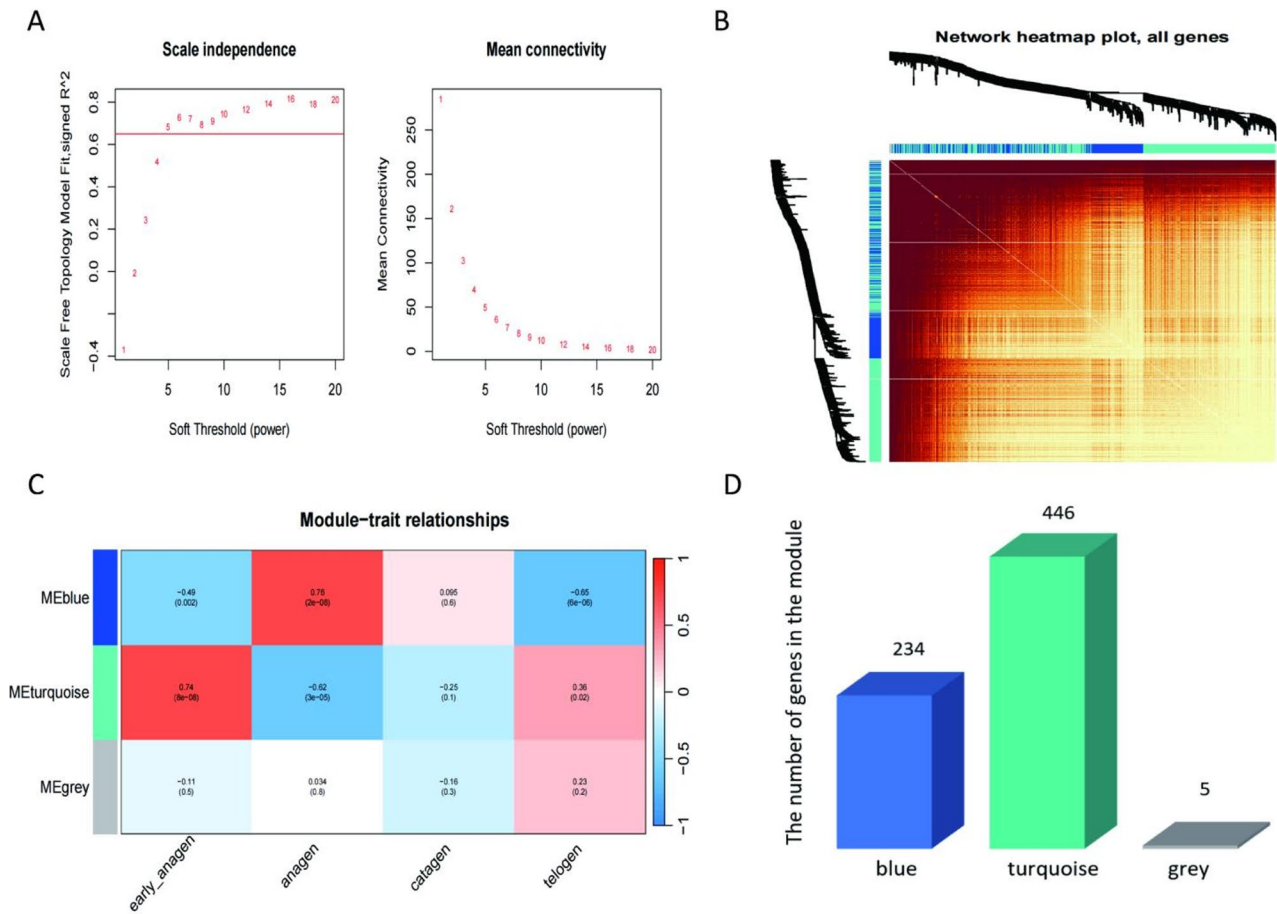


Fig. 4 WGCNA module identification. **(A)** Network topological analysis diagram with different soft-threshold values; **(B)** WGCNA heatmap; above and on the left are the gene dendrogram and corresponding bar graphs of gene modules (bright bands of different colors represent different gene modules). A cluster of highly correlated gene modules corresponds to a branch of the dendrogram; **(C)** Quantitative correlation diagram between gene modules and samples. Each row corresponds to a module feature gene, and each column corresponds to a sample. Each cell contains the respective correlation and p-value; **(D)** Statistical chart of the number of genes contained in key gene clusters

biosynthetic processes, and substance transport processes. Additionally, they were involved in 70 KEGG pathways (Fig. 6B, Table S12), including pathways such as Thyroid hormone synthesis, Oxytocin, Wnt, and TGF- β signaling pathways. These pathways were further categorized into five major classes: Metabolism, Environmental Information Processing, Cellular Processes, Organismal Systems, and Human Diseases.

Validation of RNA-seq results by RT-qPCR

In order to confirm the quality of the RNA-seq analysis, we randomly selected six lncRNAs and six mRNAs for RT-qPCR validation (Fig. 7A, B). The results indicate that the correlation coefficient between the RNA-seq and RT-qPCR results for the validated genes is above 0.9 ($R^2=0.8208$, p-value<0.01), suggesting the sequencing data used in this study is truly reliable.

Discussion

lncRNAs play diverse fundamental roles in biological processes such as chromatin remodeling, gene expression and cell growth and development, but their expression profiles and functions in HF development and cycle are still little explored. Wu et al. focused on identifying mRNAs and lncRNAs involved in secondary hair follicle (SHF) development and cycling in cashmere goats under natural conditions and provided valuable insights into lncRNA expression during SHF development [19]. Ma et al. characterized lncRNA expression profiles in hair follicles of Inner Mongolian cashmere goats at different embryonic stages [52]. Wang et al. identified lncRNA MSTRG.20890.1 as a regulator of secondary hair follicle morphogenesis and development through the chi-miR-24-3p/ADAMTS3 signaling axis [53]. Our study integrates RNA-seq data with gene network analysis to reveal lncRNA-mRNA networks that drive the transition of hair follicles into the anagen phase under shortened photoperiod conditions. We analyzed the RNA-seq

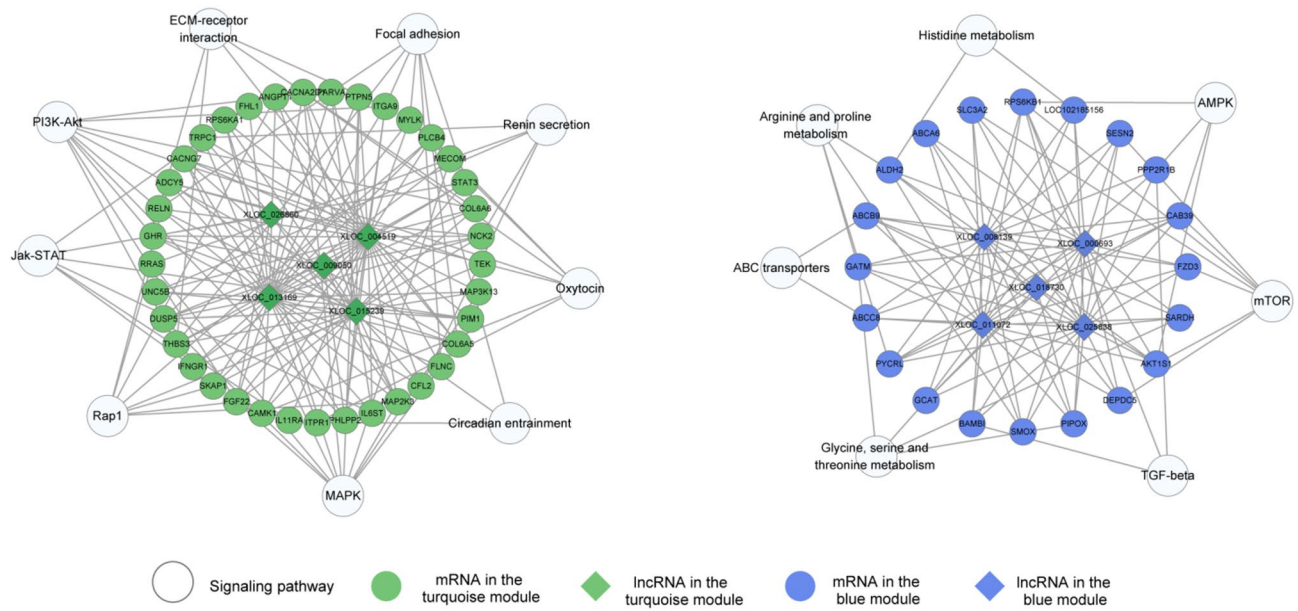


Fig. 5 Pathway-mRNA-lncRNA co-expression network

Table 1 The key module hub lncRNA

Module blue	Module turquoise
XLOC_018730	XLOC_009050
XLOC_008139	XLOC_026860
XLOC_000693	XLOC_004519
XLOC_025838	XLOC_015239
XLOC_011072	XLOC_013169

Table 2 Cis-target gene of hub lncRNA

lncRNA	Cis target gene
XLOC_018730	<i>DLX3</i> [35], <i>KAT7</i> [36]
XLOC_015239	<i>ELF3</i> [37]
XLOC_009050	<i>LPAR1</i> [38]

dataset of 39 Cashmere goat skin samples including all

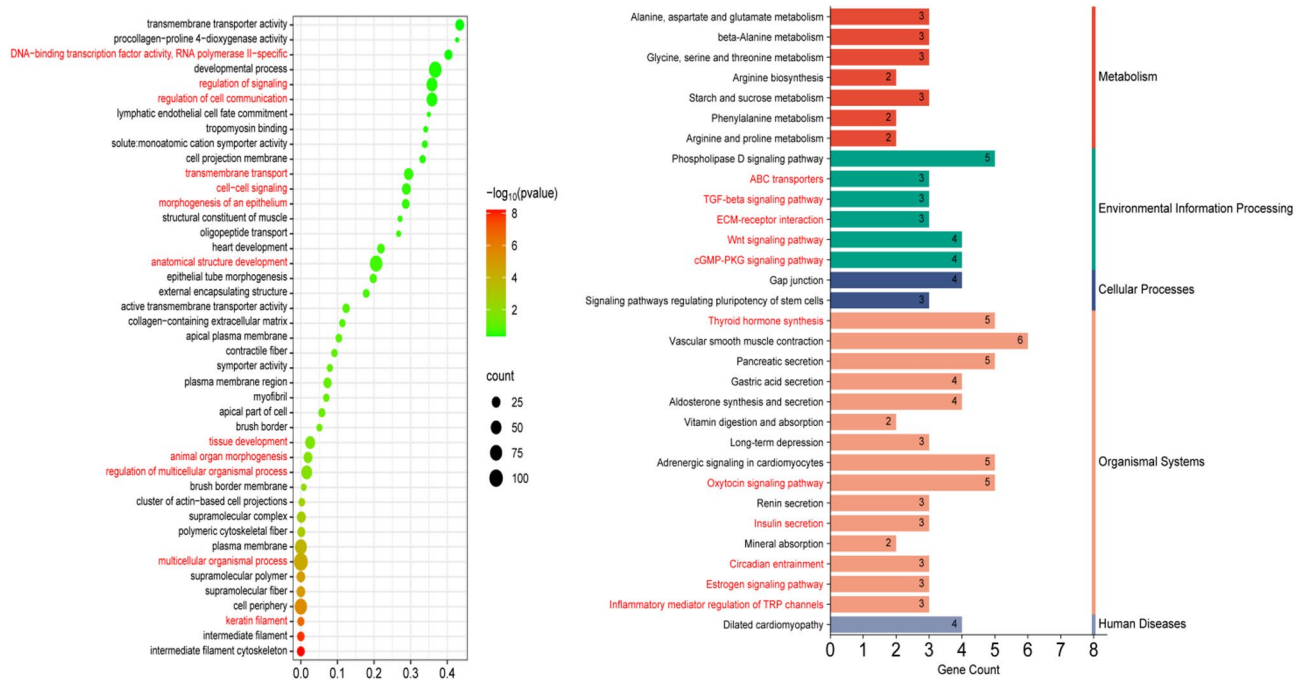


Fig. 6 Functional enrichment analysis on both the cis- and trans-target genes of the hub lncRNAs. (A) GO analysis of target genes of hub lncRNAs; (B) KEGG analysis of target genes of hub lncRNAs

Table 3 *Trans*-target gene of hub lncRNA

lncRNA	trans-target genes
XLOC_018730	<i>DLX3</i> [35], <i>ELF3</i> [37], <i>TERT</i> [39], <i>CTPS1</i> [40], <i>KRT38</i> [41]
XLOC_008139	<i>SOX6</i> [42], <i>COL22A1</i> [43], <i>IL34</i> [44]
XLOC_009050	<i>EGFL6</i> [45]
XLOC_000693	<i>DLX3</i> [35], <i>ELF3</i> [37], <i>PADI4</i> [46], <i>ABCC8</i> [47]
XLOC_025838	<i>BAMBI</i> [48], <i>TERT</i> [39], <i>VDR</i> [49], <i>CHAC1</i> [50]
XLOC_011072	<i>PADI4</i> [46]
XLOC_013169	<i>PADI4</i> [46], <i>ABCC8</i> [47]
XLOC_015239	<i>CCL20</i> [51]

growth stages and identified 1,591 lncRNAs, exhibiting stage-specific expression patterns. The significant expression changes of lncRNAs across different HF cycles underscore their pivotal role in the periodic development of HF. Furthermore, 3,412 protein-coding genes and 244 lncRNAs showed differential expression during

the HF development cycle, while 1,378 protein-coding genes and 131 lncRNAs exhibited differential expression between the shortened photoperiod and the control group. It is noteworthy that 68% of light-responsive 685 genes exhibit similar expression trends during the transition I (early anagen to anagen). The findings suggest that the process through which light control prompts hair follicles to transition prematurely from the early anagen to anagen closely mirrors the mechanism observed during the transition I. According to the results of the WGCNA analyses, it is inferred that two gene clusters associated with major signal transduction pathways that control HF development and cycling processes, specifically those associated with the blue and turquoise modules, might play a role in orchestrating the transition of the HF cycle.

In our investigation, we focused on the intricate process HF cycling, which exhibits seasonal patterns in

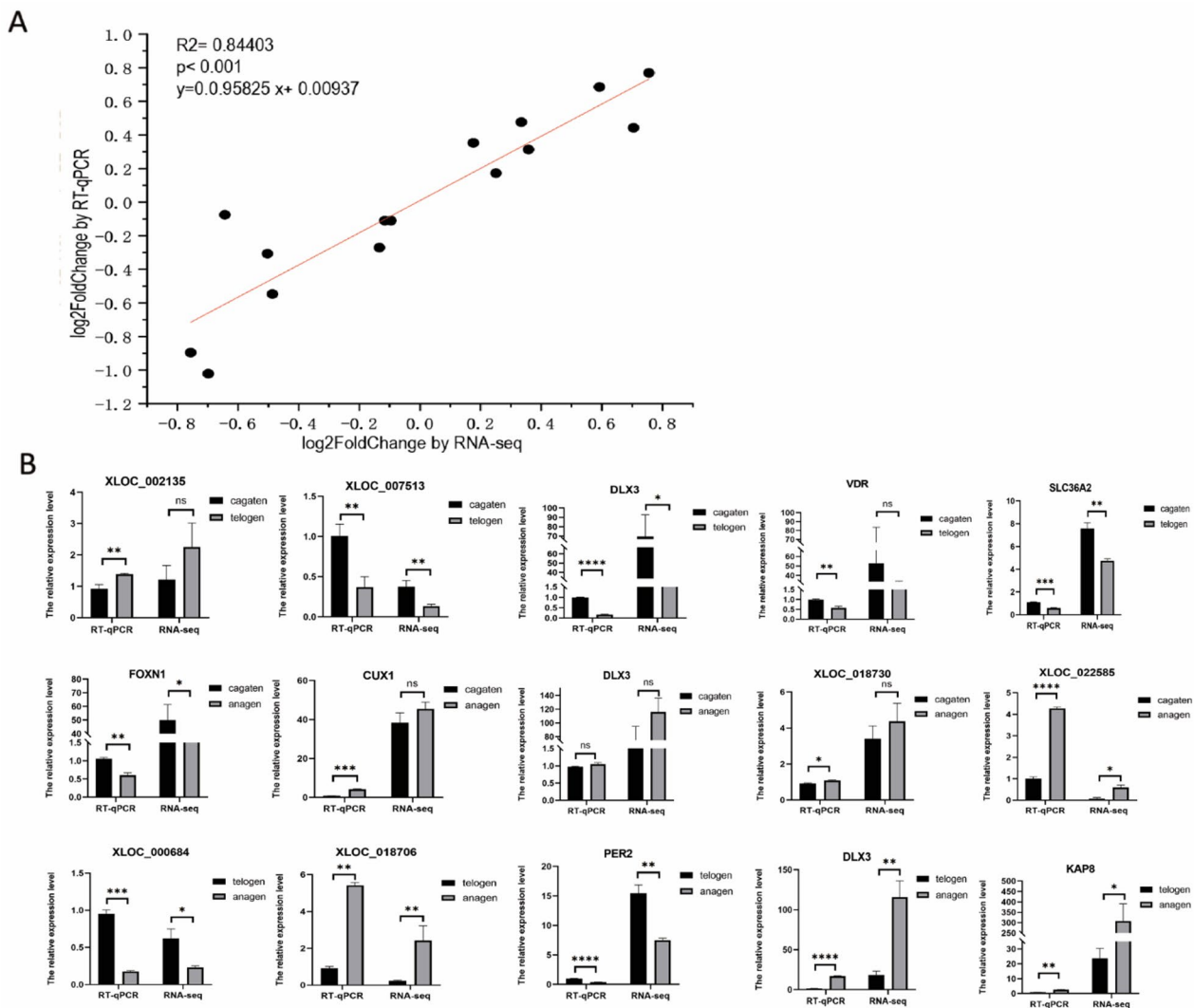


Fig. 7 Validation of RNA-seq results by RT-qPCR. **(A)** Linear correlation between RNA-seq and RT-qPCR data was presented with a log₂ fold change transformation; **(B)** The selected lncRNAs and the protein-coding genes were detected by RT-qPCR and RNA-seq (**p* < 0.05 in an un-paired t-test)

numerous mammals including horse, yak, rabbit, goat and sheep [9, 21, 22, 52, 54]. The HF cycling process is intricate, involving interactions among numerous signal pathways. To analyze the gene expression regulatory mechanisms during different stages of the HF cycle in response to shortened light exposure, we employed WGCNA on DEGs exhibiting periodic expression patterns. Within this study, we pinpointed two gene clusters, residing in the blue and turquoise modules, significantly associated with cashmere growth. The turquoise module is linked to early anagen, while the blue module predominantly relates to anagen. The turquoise module encompasses several genes, including *FGF22* [55], *DLX3* [35], *FZD1* [56], *KRT6A* [41], *ABCC9* [57], *ATG5* [58], *STAT3* [59], *CHAC1* [50], *EGFL6* [45], *FAM83G* [60], *GSDMA* [61], *ARNTL2/BMAL2* [62], known to be involved in hair follicle formation and cycle regulation. These genes primarily engage in the AMPK, mTOR, TGF- β , and ABC transporters signaling pathways. Many studies have confirmed that the mammalian target of rapamycin (mTOR) signaling pathway is essential for regulating the HF cycle [63, 64]. Similarly, the blue module harbors genes like *BAMBI* [48], *ABCC8* [47], *FZD3* [65], *ALDH2* [66], *VDR* [49], *CERS4* [67], *CLDN11* [68], *EDNRB* [69] and *GAS6* [70], associated with hair follicle formation and cycle regulation. These genes participate in ECM-receptor interaction, MAPK, Oxytocin, Jak-STAT, Rap1, and PI3K-Akt signaling pathways. The previous related studies WNT/ β -catenin, mTORC1, ERK/ MAPK, Hedgehog, TGF β signaling pathways playing important in hair follicle development and cycling for Cashmere goat [52, 53]. Consequently, these two gene clusters are likely contributors to the transition of the hair follicle cycle, potentially inducing HF to enter the anagen in advance.

lncRNAs can act as key regulators by recruiting regulatory complexes to modulate local gene expression, particularly influencing nearby genes. Notably, our study identified hub lncRNAs, namely *lnc-XLOC_025838*, *lnc-XLOC_018730*, and *lnc-XLOC_009050*, which exhibit a positive correlation with TGF- β -related genes *BAMBI*, *PPP2R1B*, and *ACVR1C*, respectively. It is worth noting that the downregulation of *BAMBI* expression has been linked to the activation of the TGF- β pathway and concurrent inhibition of the Wnt signaling pathway. Conversely, elevated *BAMBI* expression has been associated with the activation of Wnt pathways [71]. The intricate interplay between Wnt and TGF- β pathways is well-established in influencing cell proliferation and differentiation [72]. In our findings, following a shortened light exposure, we observed an increase in the expression of *DLX3*, *CTPS1*, *ELF3*, *TERT*, *KRT38*, *BAMBI*, and *VDR*. Significantly, *lnc-XLOC_018730* was predicted to target *DLX3* through both *cis*- and *trans*-acting mechanisms. *DLX3* lies within 100 kb downstream of

lnc-XLOC_018730, suggesting a potential *cis*-regulatory relationship. *lnc-XLOC_018730* may regulate nearby genes (*cis*-acting) or chromatin states, and/or exert *trans*-acting functions across the nucleus, such as modulating 3D chromosomal architecture, chromatin modification, RNA transcription, alternative splicing, nucleolar organization, or mRNA degradation [73]. The expression patterns of these hub lncRNAs aligned with those of genes associated with hair follicle development. This alignment suggests that these lncRNAs may play a role in promoting cashmere growth, potentially contributing to the premature entry of hair follicles into the anagen.

The circadian clock plays a crucial role in governing an organism's metabolic and physiological functions. Circadian genes exhibit heterogeneous expression in HFs. These genes actively contribute to the regulation of the hair cycle, aging of hair, and the production of pigment in HFs. The HF of Cashmere goats provide an exceptional model for investigating the molecular mechanisms that underlie cyclic hair growth and circadian rhythm traits [74]. Previous study showed that the secondary hair follicle of Cashmere goat can grow in advance by exposure to short photoperiod [75-76]. Therefore, shortened photoperiod treatment was an effective way to improve the growth rate, length of Cashmere goats. In our recent investigation, we observed that one month after exposure to shortened light durations, June exhibited the highest number of DEGs. This finding suggests that June holds particular significance in the regulation of cashmere growth through shortened photoperiod. Changes in photoperiods led to an advancement in the HF cycle, with alterations in the expression of numerous HF cycle-related genes, including *CLOCK* genes. Prior research has demonstrated that *CLOCK*-regulated genes experience a significant upregulation during the telogen phase. Lin et al. [11] emphasized the essential roles of *CLOCK* and *BMAL1* in regulating the HF cycle. Zhang et al. [9] further validated the expression of clock genes *BMAL1*, *CLOCK*, and *CRY1* in goat skin. *CLOCK* was identified as crucial for potential timing mechanisms during the anagen phase of hair follicles, contributing to the regulation of hair follicle cell proliferation [77]. In our dataset, we observed a heightened expression of *ARNTL2* during the telogen phase compared to the anagen phase. Moreover, reducing the duration of light exposure coincided with a decrease in *ARNTL2* expression. The core gene *PER2* also exhibited higher expression during the telogen than the anagen. Furthermore, we identified 38 *cis*-regulatory target genes associated with hair follicle development cycles, including *XLOC_000025*, *XLOC_000497*, *XLOC_000684*, *XLOC_002135*, *XLOC_004889*, *XLOC_019096*, *XLOC_018730*, *XLOC_005296*, *XLOC_022585*, *XLOC_024856*, and *XLOC_004716*. These lncRNAs are associated with *cis*-regulatory target genes such as *CRY1*,

PER2, *PER1*, and Clock genes. Our results suggest that shortened photoperiods alter the expression patterns of *ARNTL/CLOCK* genes, thereby influencing the HF cycle through circadian clock-related pathways and ultimately inducing transitions between different hair follicle stages.

Many lncRNAs modulate HF development by targeting one or multiple signaling pathways [73]. The distinct seasonal variation in cashmere growth presents a unique opportunity to explore the intricate interplay between molecular pathways and environmental factors influencing hair growth cycles. Our findings indicate that the hub lncRNA co-expressed coding genes predominantly participate in signaling pathways such as ECM-receptor interaction, MAPK, Oxytocin, Jak-STAT, Focal adhesion, Rap1, PI3K-Akt, Thyroid hormone synthesis, and Circadian entrainment. These pathways play pivotal roles in regulating stem cell pluripotency, cytokine-cytokine receptor interaction, cell adhesion molecules (CAMs), and are critical for understanding the mechanisms behind hair follicle development. Specifically, the PI3K-Akt signaling pathway, known for its regulatory role in cell proliferation, differentiation, migration, and apoptosis [78], has been established as a key player in HF regeneration [79–80]. The interaction among extracellular matrix (ECM) receptors is crucial for tissue and organ morphogenesis [81], and in the context of cashmere goat hair follicles, ECM serves as a vital matrix for rapid growth during the hair follicle growth phase [82]. The MAPK pathway, a heterotrimeric protein activated in various cells, regulates key protein kinases involved in cellular energy metabolism, impacting cell proliferation and apoptosis [83]. Prior study indicates that the oxytocin signaling pathway may activate Ca²⁺ and MAPK signaling pathways, influencing the downstream Wnt/ β -catenin signaling pathway and ultimately affecting hair follicle development [84]. Previous research has demonstrated that inhibiting the JAK-STAT signaling pathway leads to a rapid onset of anagen and subsequent hair growth [85]. Notably, our observations reveal that the key gene STAT3 in the JAK-STAT signaling pathway is down-regulated during the anagen, upregulated during the telogen, and exhibits a sharp decrease in expression levels after shortening the photoperiod. This suggests that inhibiting JAK-STAT signaling after shortening the photoperiod induces the premature entry of hair follicles into the growth phase. These lncRNAs may play an important role in regulating the HF cycle. In this study, we identified lncRNA-XLOC_018730 as a key regulator of hair follicle cycling, with its expression strongly correlated with genes involved in cell proliferation and apoptosis. Based on our co-expression network analysis, we propose that lncRNA-XLOC_018730 may act as a molecular scaffold, recruiting transcription factors such as DLX3 to regulate the expression of target genes critical for hair follicle

development. This hypothesis is supported by studies in other systems, where lncRNAs have been shown to guide transcription factors to specific genomic loci, thereby modulating gene expression. Furthermore, our findings suggest that lncRNA-XLOC_018730 may intersect with the WNT/ β -catenin signaling pathway, a well-established regulator of hair follicle cycling. Future studies involving functional validation of lncRNA-XLOC_018730 and its interaction partners will be essential to fully elucidate its role in hair follicle biology. In summary, our study sheds light on the molecular mechanisms and environmental influences shaping the complex regulation of hair follicle development in Cashmere goats.

Conclusions

In summary, Co-expression network analysis using WGCNA was performed to identify the key lncRNAs and target genes probably participating in the transformation of hair follicle cycle, two important modules with the genes like *DLX3*, *BAMBI*, *CLDN11*, *CERS4*, *EDNRB*, *ARNTL2*, *ATG5*, *CHAC1*, *EGFL6*, *GSDMA*, *STAT3*, and *FGF22* that may play an important role in involving the hair follicle formation. Further studies are needed to elucidate the Hub lncRNA underlying this regulatory mechanism.

Abbreviations

lncRNA	Long noncoding RNA
HF	Hair follicle
PHF	Primary hair follicle
SHF	Secondary hair follicle
FPKM	Fragments Per Kilobase of exon per Million fragments mapped
GO	Gene Ontology
PCA	Principal Component Analysis
DEM	Differentially expressed mRNA
DEL	Differentially expressed lncRNA
DEG	Differentially expressed gene

Supplementary Information

The online version contains supplementary material available at <https://doi.org/10.1186/s12864-025-11675-x>.

Supplementary Material 1

Acknowledgements

Not applicable.

Author contributions

JH and YM conceived and designed the experiments. YL, MY, HA, XF, HD and QL were involved in the sampling and formal analysis. MY and YL wrote the draft with discussion support from JH, EB and GA. MY, EB and GA revised it. All authors have read and approved of the manuscript.

Funding

This research was supported by the National Natural Science Foundation of China (No. 32060745 and 31802045), International Science and Technology Cooperation Project of Shihezi University (No. GJHZ202307), the Open Project of State Key Laboratory of Animal Biotech Breeding (Grant No. 2024SKLAB 6-107).

Data availability

All data generated or analyzed during this study are included within the article and supplementary materials. The raw sequence data reported in this paper have been deposited in the NCBI Sequence Read Archive (SRA) repository, PRJNA382893, under accession numbers SRR5468457 - SRR5468471 and the Genome Sequence Archive (Genomics, Proteomics & Bioinformatics 2021) (GSA: CRA016274) that are publicly accessible at <https://ngdc.cnbc.ac.cn/gsa>.

Declarations**Ethics approval and consent to participate**

The experimental Cashmere goats were from the Inner Mongolia White Cashmere Goat Farm, located in Inner Mongolia Autonomous Region of China (latitude 38°23'N, longitude 108°07'E, altitude 1378 m) and were raised according to the Cashmere goat standard feeding practices. All animal experiments were approved by the Biology Ethics Committee of Shihezi University (approval number: A2020-34). Informed consent was obtained from all owners of the Inner Mongolia White Cashmere Goat Farm for sample collection. Permissions were formally granted by the farm prior to the study.

Consent for publication

Not applicable.

Competing interests

The authors declare no competing interests.

Received: 15 July 2024 / Accepted: 6 May 2025

Published online: 15 May 2025

References

- Lee J, Böske R, Tang PC, Hartman BH, Heller S, Koehler KR. Hair follicle development in mouse pluripotent stem Cell-Derived skin organoids. *Cell Rep*. 2018;22(1):242–54.
- Schneider MR, Schmidt-Ullrich R, Paus R. The hair follicle as a dynamic minor organ. *Curr Biology*. CB. 2009;19(3):R132–42.
- Plikus MV, Baker RE, Chen CC, Fare C, de la Cruz D, Andl T, et al. Self-organizing and stochastic behaviors during the regeneration of hair stem cells. *Sci (New York NY)*. 2011;332(6029):586–9.
- Fischer TW, Slominski A, Tobin DJ, Paus R. Melatonin and the hair follicle. *J Pineal Res*. 2008;44(1):1–15.
- Yang M, Song S, Dong K, Chen X, Liu X, Rouzi M, et al. Skin transcriptome reveals the intrinsic molecular mechanisms underlying hair follicle cycling in cashmere goats under natural and shortened photoperiod conditions. *Sci Rep*. 2017;7(1):13502.
- Lin X, Zhu L, He J, Morphogenesis. Growth cycle and molecular regulation of hair follicles. *Front Cell Dev Biology*. 2022;10:899095.
- Hu XM, Li ZX, Zhang DY, Yang YC, Fu SA, Zhang ZQ, et al. A systematic summary of survival and death signaling during the life of hair follicle stem cells. *Stem Cell Res Ther*. 2021;12(1):453.
- Gao Y, Song W, Hao F, Duo L, Zhe X, Gao C, et al. Effect of fibroblast growth factor 10 and an interacting Non-Coding RNA on secondary hair follicle dermal papilla cells in cashmere goats' follicle development assessed by Whole-Transcriptome sequencing technology. *Animals*. 2023;13:13.
- O'Brien C, Darcy-Dunne MR, Murphy BA. The effects of extended photoperiod and warmth on hair growth in ponies and horses at different times of year. *PLoS ONE*. 2020;15(1):e0227115.
- Niu Y, Wang Y, Chen H, Liu X, Liu J. Overview of the circadian clock in the hair follicle cycle. *Biomolecules*. 2023;13:7.
- Lin KK, Kumar V, Geyfman M, Chudova D, Ihler AT, Smyth P, et al. Circadian clock genes contribute to the regulation of hair follicle cycling. *PLoS Genet*. 2009;5(7):e1000573.
- Yang K, Tang Y, Ma Y, Liu Q, Huang Y, Zhang Y, et al. Hair growth promoting effects of 650 Nm red light stimulation on human hair follicles and study of its mechanisms via RNA sequencing transcriptome analysis. *Ann Dermatol*. 2021;33(6):553–61.
- Liu B, Zhao R, Wu T, Ma Y, Gao Y, Wu Y, et al. Transcriptomes reveal MicroRNAs and mRNAs in different photoperiods influencing cashmere growth in goat. *PLoS ONE*. 2023;18(3):e0282772.
- Mattick JS, Amaral PP, Carninci P, Carpenter S, Chang HY, Chen LL, et al. Long non-coding RNAs: definitions, functions, challenges and recommendations. *Nat Rev Mol Cell Biol*. 2023;24(6):430–47.
- Zhang SF, Li XR, Sun CB, He YK. [Epigenetics of plant vernalization regulated by non-coding RNAs]. *Hereditas*. 2012;34(7):829–34.
- Hu CZ, Cai L, Yu T, Zhao XY, Yang Ming. Research progress of long Non-coding RNAs in stress response to environmental pollutions. *Asian J Ecotoxicol*. 2023;18(01):39–50.
- Sulayman A, Tian K, Huang X, Tian Y, Xu X, Fu X, et al. Genome-wide identification and characterization of long non-coding RNAs expressed during sheep fetal and postnatal hair follicle development. *Sci Rep*. 2019;9(1):8501.
- Song S, Yang M, Li Y, Rouzi M, Zhao Q, Pu Y, et al. Genome-wide discovery of lincRNAs with spatiotemporal expression patterns in the skin of goat during the cashmere growth cycle. *BMC Genomics*. 2018;19(1):495.
- Wu C, Qin C, Fu X, Huang X, Tian K. Integrated analysis of lincRNAs and mRNAs by RNA-Seq in secondary hair follicle development and cycling (anagen, catagen and telogen) of Jiangnan cashmere goat (*Capra hircus*). *BMC Vet Res*. 2022;18(1):167.
- Sun H, Meng K, Wang Y, Wang Y, Yuan X, Li X. LncRNAs regulate the cyclic growth and development of hair follicles in Dorper sheep. *Front Veterinary Sci*. 2023;10:1186294.
- Zhao B, Chen Y, Hu S, Yang N, Wang M, Liu M, et al. Systematic analysis of Non-coding RNAs involved in the Angora rabbit (*Oryctolagus cuniculus*) hair follicle cycle by RNA sequencing. *Front Genet*. 2019;10:407.
- Zhang X, Bao P, Ye N, Zhou X, Zhang Y, Liang C et al. Identification of the key genes associated with the Yak hair follicle cycle. *Genes*. 2021;13(1).
- Kim D, Paggi JM, Park C, Bennett C, Salzberg SL. Graph-based genome alignment and genotyping with HISAT2 and HISAT-genotype. *Nat Biotechnol*. 2019;37(8):907–15.
- Pertea M, Pertea GM, Antonescu CM, Chang TC, Mendell JT, Salzberg SL. StringTie enables improved reconstruction of a transcriptome from RNA-seq reads. *Nat Biotechnol*. 2015;33(3):290–5.
- Kropinski AM, Clokie MR. Methods in molecular biology. Introduction. Methods in molecular biology. (Clifton NJ). 2009;502:xiii–xxii.
- Kang YJ, Yang DC, Kong L, Hou M, Meng YQ, Wei L, et al. CPC2: a fast and accurate coding potential calculator based on sequence intrinsic features. *Nucleic Acids Res*. 2017;45(W1):W12–6.
- Sun L, Luo H, Bu D, Zhao G, Yu K, Zhang C, et al. Utilizing sequence intrinsic composition to classify protein-coding and long non-coding transcripts. *Nucleic Acids Res*. 2013;41(17):e166.
- Love MI, Huber W, Anders S. Moderated Estimation of fold change and dispersion for RNA-seq data with DESeq2. *Genome Biol*. 2014;15(12):550.
- Langfelder P, Horvath S. WGCNA: an R package for weighted correlation network analysis. *BMC Bioinformatics*. 2008;9:559.
- Bindea G, Mlecnik B, Hackl H, Charoentong P, Tosolini M, Kirilovsky A, et al. ClueGO: a cytoscape plug-in to decipher functionally grouped gene ontology and pathway annotation networks. *Bioinf (Oxford England)*. 2009;25(8):1091–3.
- Shannon P, Markiel A, Ozier O, Baliga NS, Wang JT, Ramage D, et al. Cytoscape: a software environment for integrated models of biomolecular interaction networks. *Genome Res*. 2003;13(11):2498–504.
- Rao X, Huang X, Zhou Z, Lin X. An improvement of the 2⁻(-delta delta CT) method for quantitative real-time polymerase chain reaction data analysis. *Biostatistics Bioinf Biomathematics*. 2013;3(3):71–85.
- Zhang YX, Lv J, Bai JY, Pu X, Dai EL. Identification of key biomarkers of the glomerulus in focal segmental glomerulosclerosis and their relationship with immune cell infiltration based on WGCNA and the LASSO algorithm. *Ren Fail*. 2023;45(1):2202264.
- Kopp F, Mendell JT. Functional classification and experimental dissection of long noncoding RNAs. *Cell*. 2018;172(3):393–407.
- Hwang J, Mehrani T, Millar SE, Morasso MI. Dlx3 is a crucial regulator of hair follicle differentiation and cycling. *Development*. 2008;135(18):3149–59.
- Brohem CA, de Carvalho CM, Radoski CL, Santi FC, Baptista MC, Swinka BB, et al. Comparison between fibroblasts and mesenchymal stem cells derived from dermal and adipose tissue. *Int J Cosmet Sci*. 2013;35(5):448–57.
- Kowalczyk A, Chikina M, Clark N. Complementary evolution of coding and noncoding sequence underlies mammalian hairlessness. *eLife*. 2022;11.
- Wu C, Ma S, Zhao B, Qin C, Wu Y, Di J, et al. Drivers of plateau adaptability in cashmere goats revealed by genomic and transcriptomic analyses. *BMC Genomics*. 2023;24(1):428.

39. Ikeda M, Yabe S, Kiso M, Ishiguro N, Tsunemi Y, Okochi H. TERT/BMI1-transgenic human dermal papilla cells enhance murine hair follicle formation in vivo. *J Dermatol Sci*. 2022;106(2):78–85.
40. Zhang C, Li Y, Qin J, Yu C, Ma G, Chen H, et al. TMT-Based quantitative proteomic analysis reveals the effect of bone marrow derived mesenchymal stem cell on hair follicle regeneration. *Front Pharmacol*. 2021;12:658040.
41. Yu Z, Gordon SW, Nixon AJ, Bowden CS, Rogers MA, Wildermoth JE, et al. Expression patterns of keratin intermediate filament and keratin associated protein genes in wool follicles. *Differ Res Biol Divers*. 2009;77(3):307–16.
42. Zhao R, Li J, Liu N, Li H, Liu L, Yang F, et al. Transcriptomic analysis reveals the involvement of lncRNA-miRNA-mRNA networks in hair follicle induction in Aohan fine wool sheep skin. *Front Genet*. 2020;11:590.
43. Meng G, Bao Q, Ma X, Chu M, Huang C, Guo X et al. Analysis of copy number variation in the whole genome of normal-haired and long-haired tianzhu white Yaks. *Genes*. 2022;13(12).
44. Chen Y, Liu L, Fan J, Zhang T, Zeng Y, Su Z. Low-level laser treatment promotes skin wound healing by activating hair follicle stem cells in female mice. *Lasers Med Sci*. 2022;37(3):1699–707.
45. Wei JP, Gong Y, Zhong HB, Hua Wang T, Liao XH. EGFL6 expression in hair follicle central isthmus is dependent on the presence of terminal Schwann cells. *Exp Dermatol*. 2020;29(4):400–3.
46. Vikhe Patil K, Mak KH, Genander M. A hairy Cytuation - PADIs in regeneration and alopecia. *Front Cell Dev Biol*. 2021;9:789676.
47. Becker GM, Woods JL, Schauer CS, Stewart WC, Murdoch BM. Genetic association of wool quality characteristics in united States Rambouillet sheep. *Front Genet*. 2022;13:1081175.
48. Gong G, Fan Y, Yan X, Li W, Yan X, Liu H, et al. Identification of genes related to hair follicle cycle development in inner Mongolia cashmere goat by WGCNA. *Front Veterinary Sci*. 2022;9:894380.
49. Joko Y, Yamamoto Y, Kato S, Takemoto T, Abe M, Matsumoto T et al. VDR is an essential regulator of hair follicle regression through the progression of cell death. *Life Sci Alliance*. 2023;6(11).
50. Karami H, Nomiri S, Ghasemigol M, Mehrvarzian N, Derakhshani A, Fereidouni M, et al. CHAC1 as a novel biomarker for distinguishing alopecia from other dermatological diseases and determining its severity. *IET Syst Biol*. 2022;16(5):173–85.
51. Scharschmidt TC, Vasquez KS, Pauli ML, Leitner EG, Chu K, Truong HA, et al. Commensal microbes and hair follicle morphogenesis coordinately drive Treg migration into neonatal skin. *Cell Host Microbe*. 2017;21(4):467–77. e5.
52. Ma R, Shang F, Rong Y, Pan J, Wang M, Niu S, et al. Expression profile of long non-coding RNA in inner Mongolian cashmere goat with putative roles in hair follicles development. *Front Veterinary Sci*. 2022;9:995604.
53. Wang M, Ma R, Ma Q, Ma B, Shang F, Lv Q, et al. Role of lncRNA MSTRG.20890.1 in hair follicle development of cashmere goats. *Genes*. 2024;15:1392.
54. Lei Z, Sun W, Guo T, Li J, Zhu S, Lu Z et al. Genome-wide selective signatures reveal candidate genes associated with hair follicle development and wool shedding in sheep. *Genes*. 2021;12(12).
55. Beyer TA, Werner S, Dickson C, Grose R. Fibroblast growth factor 22 and its potential role during skin development and repair. *Exp Cell Res*. 2003;287(2):228–36.
56. He J, Zhao B, Huang X, Fu X, Liu G, Tian Y, et al. Gene network analysis reveals candidate genes related with the hair follicle development in sheep. *BMC Genomics*. 2022;23(1):428.
57. Ohko K, Nakajima K, Nakajima H, Hiraki Y, Kubota K, Fukao T, et al. Skin and hair abnormalities of Cantu syndrome: A congenital hypertrichosis due to a genetic alteration mimicking the Pharmacological effect of Minoxidil. *J Dermatol*. 2020;47(3):306–10.
58. Cai B, Zheng Y, Yan J, Wang J, Liu X, Yin G. BMP2-mediated PTEN enhancement promotes differentiation of hair follicle stem cells by inducing autophagy. *Exp Cell Res*. 2019;385(2):111647.
59. Miyauchi K, Ki S, Ukai M, Suzuki Y, Inoue K, Suda W, et al. Essential role of STAT3 signaling in hair follicle homeostasis. *Front Immunol*. 2021;12:663177.
60. Balmer P, Fellay AK, Sayar BS, Hariton WVJ, Wiener DJ, Galichet A, et al. FAM83G/Fam83g genetic variants affect canine and murine hair formation. *Exp Dermatol*. 2019;28(4):350–4.
61. Lin PH, Lin HY, Kuo CC, Yang LT. N-terminal functional domain of gasdermin A3 regulates mitochondrial homeostasis via mitochondrial targeting. *J Biomed Sci*. 2015;22(1):44.
62. Coltery A, Browne JA, O'Brien C, Sheridan JT, Murphy BA. Optimised stable lighting strengthens circadian clock gene rhythmicity in equine hair follicles. *Animals*. 2023;13:14.
63. Tu W, Cao YW, Sun M, Liu Q, Zhao HG. mTOR signaling in hair follicle and hair diseases: recent progress. *Front Med*. 2023;10:1209439.
64. Deng Z, Lei X, Zhang X, Zhang H, Liu S, Chen Q, et al. mTOR signaling promotes stem cell activation via counterbalancing BMP-mediated suppression during hair regeneration. *J Mol Cell Biol*. 2015;7(1):62–72.
65. Hung BS, Wang XQ, Cam GR, Rothnagel JA. Characterization of mouse Frizzled-3 expression in hair follicle development and identification of the human homolog in keratinocytes. *J Invest Dermatol*. 2001;116(6):940–6.
66. Lee S, Ohn J, Mi Kang B, Tommy Hwang S, Kwon O. Activation of mitochondrial aldehyde dehydrogenase 2 promotes hair growth in human hair follicles. *J Adv Res*. 2023;64:237–247.
67. Peters F, Vorhagen S, Brodessaer S, Jakobshagen K, Brüning JC, Niessen CM, et al. Ceramide synthase 4 regulates stem cell homeostasis and hair follicle cycling. *J Invest Dermatol*. 2015;135(6):1501–9.
68. Troy TC, Turksen K. The targeted overexpression of a Claudin mutant in the epidermis of Transgenic mice elicits striking epidermal and hair follicle abnormalities. *Mol Biotechnol*. 2007;36(2):166–74.
69. Li H, Fan L, Zhu S, Shin MK, Lu F, Qu J, et al. Epilation induces hair and skin pigmentation through an EDN3/EDNRB-dependent regenerative response of melanocyte stem cells. *Sci Rep*. 2017;7(1):7272.
70. Fan X, Zhao X, Xu J, Wang J, Wang Q, Tang X. Triton modified polyethyleneimine conjugates assembled with growth arrest-specific protein 6 for androgenic alopecia transdermal gene therapy. *Mater Today Bio*. 2023;19:100575.
71. Oshimori N, Fuchs E. Paracrine TGF- β signaling counterbalances BMP-mediated repression in hair follicle stem cell activation. *Cell Stem Cell*. 2012;10(1):63–75.
72. Attisano L, Wrana JL. Signal integration in TGF- β , WNT, and hippo pathways. *F1000Prime Rep*. 2013;5:17.
73. Kopp F, Mendell JT. Functional classification and experimental dissection of long noncoding RNAs [J]. *Cell*. 2018;172(3):393–407.
74. Liu LP, Li MH, Zheng YW. Hair follicles as a critical model for monitoring the circadian clock. *Int J Mol Sci*. 2023;24(3).
75. Zhang CZ, Sun HZ, Li SL, Sang D, Zhang CH, Jin L, et al. Effects of photo-period on nutrient digestibility, hair follicle activity and cashmere quality in Inner Mongolia white cashmere goats. *Asian-Australas J Anim Sci*. 2019;32(4):541–547.
76. Li J, Tian G, Wang X, Tang H, Liu Y, Guo H, et al. Effects of short photo-period on cashmere growth, hormone concentrations and hair follicle development-related gene expression in cashmere goats. *J Appl Anim Res*. 2023;51(1):52–61.
77. Zhang W, Wang N, Zhang T, Wang M, Ge W, Wang X. Roles of melatonin in goat hair follicle stem cell proliferation and pluripotency through regulating the Wnt signaling pathway. *Front Cell Dev Biol*. 2021;9:686805.
78. Samakova A, Gazova A, Sabova N, Valaskova S, Jurikova M, Kyselovic J. The PI3k/Akt pathway is associated with angiogenesis, oxidative stress and survival of mesenchymal stem cells in pathophysiologic condition in ischemia. *Physiol Res*. 2019;68(Suppl 2):S131–8.
79. Grosbois J, Demeestere I. Dynamics of PI3K and Hippo signaling pathways during in vitro human follicle activation. *Hum Reprod (Oxford England)*. 2018;33(9):1705–14.
80. Chen Y, Fan Z, Wang X, Mo M, Zeng SB, Xu RH, et al. PI3K/Akt signaling pathway is essential for de Novo hair follicle regeneration. *Stem Cell Res Ther*. 2020;11(1):144.
81. Xu T, Guo X, Wang H, Hao F, Du X, Gao X, et al. Differential gene expression analysis between anagen and Telogen of *Capra hircus* skin based on the de Novo assembled transcriptome sequence. *Gene*. 2013;520(1):30–8.
82. Zhu B, Xu T, Yuan J, Guo X, Liu D. Transcriptome sequencing reveals differences between primary and secondary hair follicle-derived dermal papilla cells of the cashmere goat (*Capra hircus*). *PLoS ONE*. 2013;8(9):e76282.
83. Ren XH, Wang WP. Autophagy in Cancer chemoresistance. *Chin J Biochem Mol Biology*. 2015;31(05):448–54.
84. Gao Y, Duo L, Zhe X, Hao L, Song W, Gao L, et al. Developmental mapping of hair follicles in the embryonic stages of cashmere goats using proteomic and metabolomic construction. *Animals*. 2023;13:19.
85. Harel S, Higgins CA, Cerise JE, Dai Z, Chen JC, Clynes R, et al. Pharmacologic Inhibition of JAK-STAT signaling promotes hair growth. *Sci Adv*. 2015;1(9):e1500973.

Publisher's note

Springer Nature remains neutral with regard to jurisdictional claims in published maps and institutional affiliations.